Chapter 2

Fundamentals of Electric Spring and its System Design

2.1 Introduction

Rapid urbanization, industrial growth, and ever-increasing population have tremendously resulted in the increased demand for electricity. Any nation's development can always be linked with the per capita consumption of electricity [57]. This increased demand for electricity can only be commensurated by enhancing the generation capabilities up to some feasible extent, beyond which it has its economic and environmental repercussions. Conventionally, electricity generation has extensively depended on fossil-based resources (e.g., Coal) and sustainable energy sources (e.g., Nuclear). The rapid growth of the energy sector has started depleting non-renewable and fossil-based energy sources and has caused considerable damage to the environment due to greenhouse gas emissions. Stringent environmental treaties (viz. Kyoto protocol) have enforced the signatory nations to put a break on to the carbon emission to prevent the damage to the environment beyond an irrecoverable extent or a point of no return.

These factors have opened up new avenues in the sector of energy generation using RES through DGs, and conservation using FACTS, CPDs, and DSM.

2.2   Impact of Integration of Renewables

Environmental treaties like the Kyoto protocol talk about reducing the emission of green-house gases and managing the existing infrastructure efficiently, curtailing the emitting sources of electricity generation, and proliferating the use of sustainable and renewable energy sources (RES) [58] viz., wind and solar, for the generation of electricity through distributed generation (DG), without incurring any wheeling cost that too without adversely impacting the environment. The integration of RES into the distribution grid has a detrimental impact on the electrical system, as it causes oscillations and disturbances [59], hampering the steady-state stability of the power system [60], due to its intermittent and unpredictable nature. In a way, the integration of RES pollutes the electrical power. Furthermore, the unpredictability of RES creates issues in the day ahead forecasting, scheduling, and bidding of the power, in the new regime of the restructured/unbundled power system [61].

There has to be a system that could avert the ill effects of voltage fluctuation caused due to the inclusion of RES in the distribution grid, and further, this could affirm the expected and satisfactory operation of electrical equipment connected with it. ES is the plausible answer to the problems associated with the issue of poorly regulated voltage due to the heuristic nature of RES, and at the same time, ES is providing the DSM in real-time.

2.3   Concept of Electric Spring

ES is named so because it mimics its mechanical counterpart's action, which absorbs the thrust or impact onto it, and the same can be explained using Hook's law. A similarity in the action of ES with that of a mechanical spring can be explained from Fig. 2.1. ES provides the voltage regulation and minimizing the oscillations caused by the intermittency of the DGs.

ES is a current-controlled voltage source converter (VSC), also referred to as a CPD [62] due to its smaller rating, that can ameliorate the adverse impact of RES and help improve the DSM at the consumer's end. It is worth noting that a load of any system can always be bifurcated or categorized into critical one and non-critical one, depending on the requirement of controlled and well-regulated voltage. ES is a VSC that has been
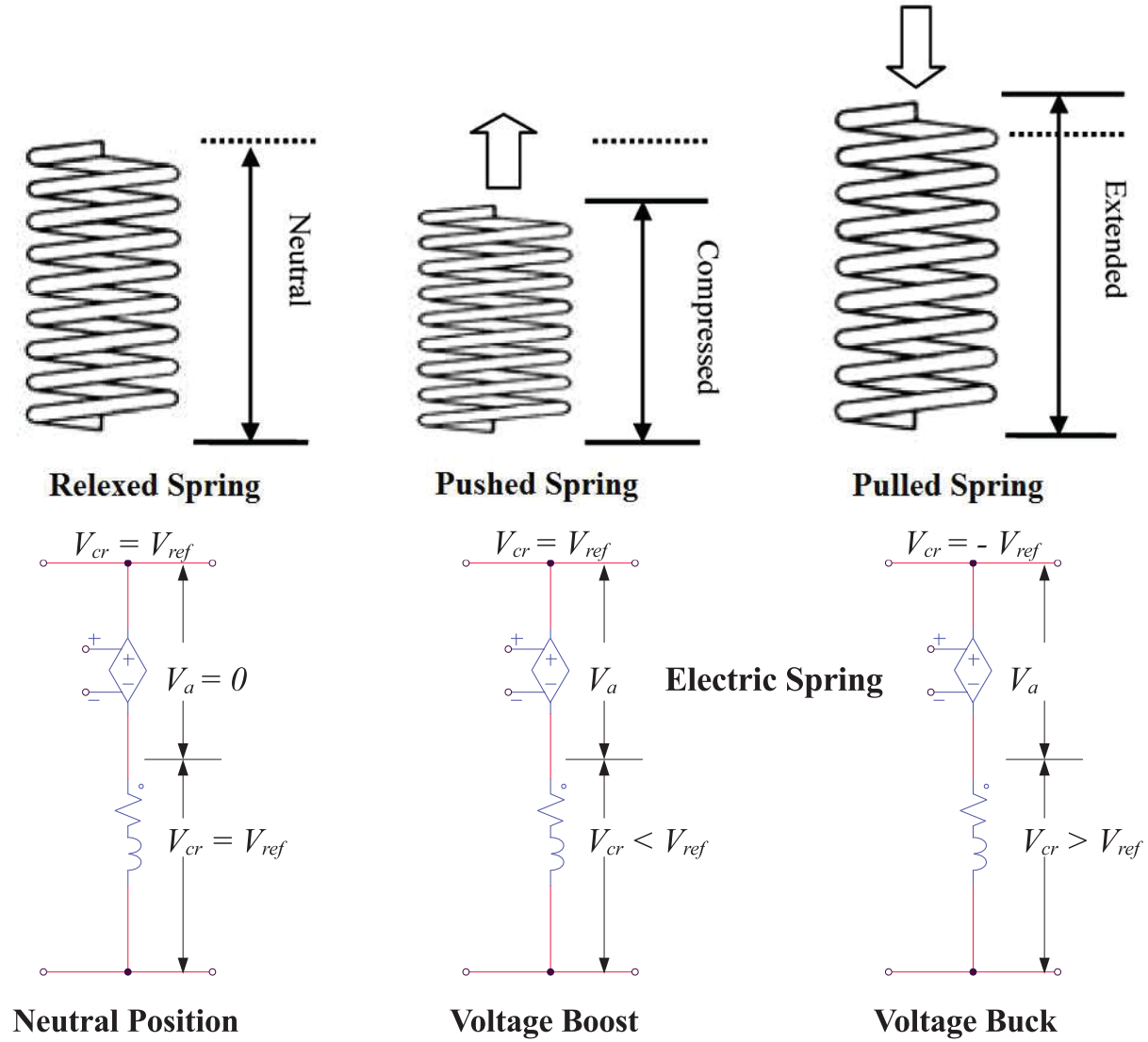
Figure 2.1: Functional Evaluation of Mechanical Spring and Electrical Spring.

connected in series with the dissipative load (heating, ventilating, and air conditioning (HVAC) and lighting loads, and tolerant to fluctuating supply), also referred to as non-critical load (NC). Together this combination (ES and NC) is constituting a smart load, which further is connected across the critical load, which is very sensitive to fluctuations in the voltage (e.g., data centers, hospital's surgical types of equipment, etc.). This combination of smart load and the critical load is being catered by the utility grid. This arrangement can readily be implemented in large as well as small residential / commercial buildings [63] [64]. Heating and lighting load constitutes about 68% of the total load of the building [63] and can be regarded as a non-critical load. ES changes the voltage of NC

load and its power flow, even when load and supply voltage is unchanged. It does so by injecting the voltage in quadrature or phase or at some angle in between, with respect to the reference quantity phase, and hence providing active and / or reactive power support. *ES* is acting as a buffer between load and source, as shown in Fig:2.2, very much like its mechanical counterpart, hence named so.

ES's dispersed through the distribution system can source or sink the active as well as reactive power and provide voltage regulation and hence stability to the grid, in a manner similar to an array of mechanical springs giving support to a mattress, and thus consolidating its name as electric spring, using the mechanism of droop control and without resorting to the use of Internet and Communication Technology (ICT) for the coordinated management of multiple *ES*.
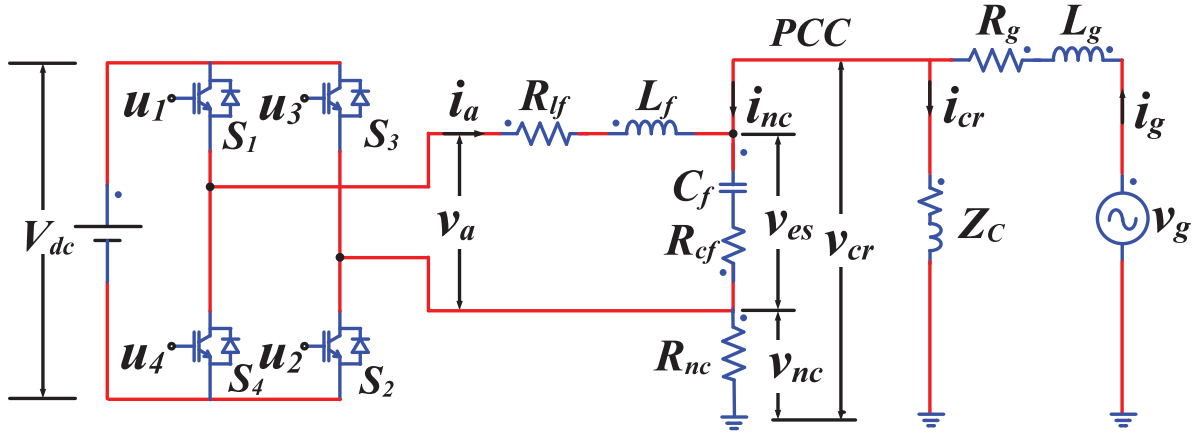

Figure 2.2: System of ES, Comprising of Smart Load and Critical Load.

2.3.1 Evolution and Configurations of Electric Spring

Ever since the inception of the *ES* [6], it has also evolved by accommodating various configurational changes. This evolution can be presented in the form of different generations viz., 1st, 2nd, and 3rd generation of *ES*.

1st and 2nd generation *ES* works better to prevent under-voltage than to suppress over-voltage; further, its voltage regulating ability greatly depends on the characteristics of the load. 3rd generation *ES*, with a back-to-back converter configuration, works better to overcome the limitations of 1st and 2nd generation *ES* by extending the operational flexibility [65]. 3rd generation *ES* lacks reliability due to the additional converter to be

controlled, tackling with the bidirectional exchange of power, and restricting the prolif-
eration of harmonics to the grid as prescribed by the standards viz., IEEE-519 [66]. No
surprise to see only a handful of technical publications on 1st and 3rd generation ES, and
the presence of a large number of publications on the 2nd generation ES. 2nd generation
ES offers more operational flexibility in terms of voltage support (by active and reactive
power support) with more reliability, and hence this work has a focus on the 2nd gener-
ation ES. ES emanates voltage (v_{es}) so as to bridge the gap between the difference of
voltage being supported by the non-critical load (v_{nc}) and that demanded by the critical
load (v_c), i.e.,

$$v_c = v_{nc} + v_{es} \tag{2.1}$$

The Control system of ES is the key to the successful generation of the desired voltage
(v_c), across the critical load, by injecting v_{es} having an appropriate phase and magnitude
through ES. Numerous methods of generating v_{es} have nicely been presented and ex-
plained through phasers in [67] for the application of micro-grid. A brief state-of-art
overview of the controllers has already been presented in Chapter:1.

2.3.2   Precursor on the Control of Electric Spring

This work has been focused on the control aspect and its implication on 2nd Generation
ES as an efficient mechanism of low-cost real-time Demand-Side management. A math-
ematical model of ES, using the state-space method with the system being considered a
multivariable one, has been used to design various controllers being verified in this work.
The considered model possesses numerous uncertainties viz., variation in DC bus voltage,
Load change, change in grid voltage, and change in cable length causing a change in the
cable's conductors impedance. The designed controller has to have enough robustness to
combat these variations and uncertainties, presented next.

2.4   System of Electric Spring

The state-space method has been adopted for carrying out the mathematical model of
the system, shown in Figure. 2.2. For the sake of simplifying the model and further
minimizing the burden of calculations in the design intricates of the controller, Equivalent

series resistance (ESR) of L_f and internal resistance of C_f (i.e. R_{lf} and R_{cf}) have been neglected, as can be depicted in Figure. 2.3. Further, both non-critical and critical load has been considered as purely resistive, for the sake of modeling and controller design to reduce the order of the system (which otherwise could assume any of the load type, as mentioned in Sect. 2.7 and corresponding simulation test bench).
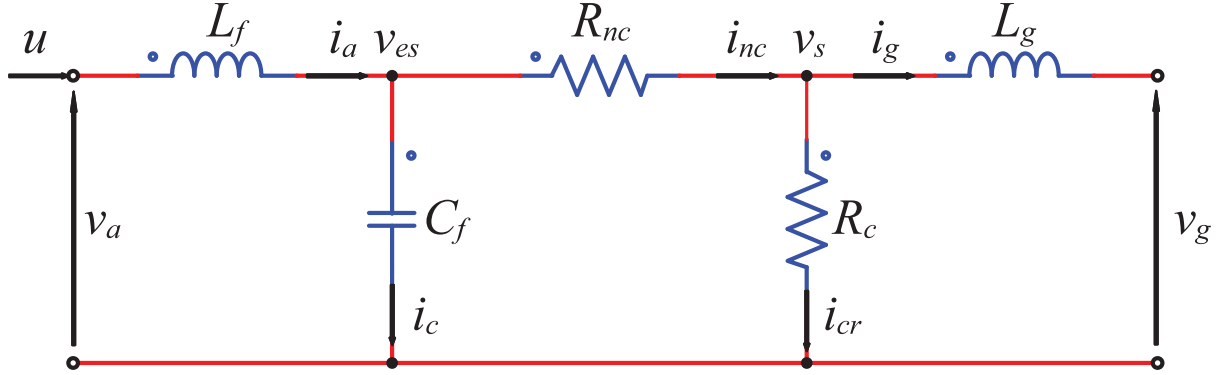

Figure 2.3: System of ES Considered Considered as a Network for the Execution of Mathematical Model.

2.4.1 Model Intricate and Uncertainties

There exist numerous uncertainties in the system considered (Figure. 2.2) due to the change in the system parameters, which could alter the derived model. These uncertainties are detailed as follows:

- Grid voltage - v_g, varies within the permissible limits of $[v_{g(max)} \quad v_{g(min)}]$.

- Grid impedance - Z_g, varies according to the feeder length and type of the conductor used there in, and this makes variation in $L_g[L_{g(max)} \quad L_{g(min)}]$ and in $R_g[R_{g(max)} \quad R_{g(min)}]$.

- Critical and non-critical loads, have been varied within the prescribed bounds of $[R_{c(max)} \quad R_{c(min)}]$ and $[R_{nc(max)} \quad R_{nc(min)}]$. Further, critical load assumes any of the load variants (to be of R, R-L, or R-C type). Switching to a particular load variant may altogether change the order of the modeled system.

- Voltage of the DC bus - V_{dc}, varies depending on the generation of *ES*.

    1. 1st generation *ES*, has a variable and pulsating voltage having large peaks, due to variable grid voltage, and this has to be brought within the limits.

    2. 2nd generation *ES*, has variable battery potential depending on the demand of the connected load.

    3. 3rd generation *ES*, has ever changing DC bus voltage due to variation in demand and supply of the voltage.

- Control system needs to vary the modulation index m in the prescribed bound of [-1 1], so as to maintain the voltage v_{cr} constant.

Incorporating parametric changes in the assumed model of the system makes it a complex system to be analyzed (as it happens to be a polytopic model [68], with 2^6 vertices (maximum possibilities)) using Linear Programming approach [69]. This complex polytopic model could be made simpler; by transforming it into a monotopic one.

2.4.2   Model of Electric Spring

The considered system is a MIMO system with u as a control input (v_a being controlled by the controller's output - u) and grid voltage v_g, as disturbance input. The mathematical model of the system shown in Fig:2.3, has been derived by implementing KCL and KVL on it. The following equations have been deduced, leading to the final state-space model. Average switched model [70][71][72] has been considered, for the reason that the switching frequency ($f_{sw} = 20KHz$) considered here is significantly higher than the supply frequency ($f_s = 50Hz$) of the grid voltage.

$$\frac{di_a}{dt} = \dot{i_a} = \frac{1}{L_f}(-v_{es} + v_a); \tag{2.2}$$

$$\frac{di_g}{dt} = \dot{i_g} = \frac{1}{L_g}(v_g - v_{es} + i_{nc}R_{nc}); \tag{2.3}$$

$$\frac{dv_{es}}{dt} = \dot{v_{es}} = \frac{1}{C_f}(i_a - i_{nc}); \tag{2.4}$$

$$i_{nc} = \frac{v_{es}}{R_c + R_{nc}} - \frac{R_c i_g}{R_c + R_{nc}} \tag{2.5}$$

Substituting the value of i_{nc} from (2.5) into (2.3) and (2.4) yields state-space model of the system as,

$$\dot{x}(t) = A.x(t) + B_1.v_a(t) + B_2.v_g(t),$$
$$= A.x(t) + B.U(t),$$
$$y(t) = C.x(t) + D.U(t),$$

$$\begin{bmatrix} \dot{x}(t) \\ y(t) \end{bmatrix} = \begin{bmatrix} A & B \\ C & D \end{bmatrix} \begin{bmatrix} x(t) \\ U(t) \end{bmatrix}$$

$$\begin{bmatrix} \dot{v}_{es} \\ \dot{i}_a \\ \dot{i}_g \end{bmatrix} = \begin{bmatrix} -\frac{1}{C_f(R_c+R_{nc})} & -\frac{1}{C_f} & \frac{R_c}{C_f(R_c+R_{nc})} \\ \frac{1}{L_f} & 0 & 0 \\ -\frac{R_c}{L_g(R_c+R_{nc})} & 0 & -\frac{R_cR_{nc}}{L_g(R_c+R_{nc})} \end{bmatrix} \begin{bmatrix} v_{es} \\ i_a \\ i_g \end{bmatrix} + \begin{bmatrix} 0 & 0 \\ \frac{1}{L_f} & 0 \\ 0 & \frac{1}{L_g} \end{bmatrix} \begin{bmatrix} v_a \\ v_g \end{bmatrix}$$

$$v_s = \begin{bmatrix} \frac{R_c}{(R_c+R_{nc})} & 0 & \frac{R_cR_{nc}}{(R_c+R_{nc})} \end{bmatrix} \begin{bmatrix} v_{es} \\ i_a \\ i_g \end{bmatrix} + \begin{bmatrix} 0 & 0 \end{bmatrix} \begin{bmatrix} v_a \\ v_g \end{bmatrix}$$

$$(2.6)$$

Where,

$$x(t) = [v_{es}(t) \quad i_f(t) \quad i_g(t)]^T,$$
$$B = [B_1 \quad B_2],$$
$$U(t) = [v_a(t) \quad v_g(t)]^T,$$
$$u(t) = m.sin(\omega t + \delta),$$
$$v_a(t) \cong V_{dc}.u(t) \quad \text{(assuming that higher order harmonics are absent)},$$

m, is modulation index $\in [-1, 1]$,

δ, is the phase of injected voltage by ES, and

$e(t) = v_g(t) = V_m.sin(\omega t)$, the disturbance input,

$y(t) = v_{cr}(t)$, voltage across the critical load

ω, angular velocity of v_g.

Table.2.1 shows the parametric values, with corresponding limits. Substituting these varied and range of values in the derived model (2.6), leads to a Polytopic model [73][68][69], possessing 2^4 vertices (due to change in V_{dc}, Z_c, Z_g and v_g). Use of a polytopic model so derived would be adding unnecessary complications in the controller design. A simple

Table 2.1: Parameters Considered in the System of ES

Parameters	Nomenclature	Upper Limit	Lower Limit
Dc Bus Voltage	V_{dc}	750V	550
Filter Inductance	L_f	2mH	-
ESR of L_f	R_{lf}	0.85Ω	-
Filter Capacitance	C_f	6μF	-
Internal resistance of C_f	R_{cf}	100Ω	-
Inductance of the Cable	L_g	0.305 mH	1.00 mH
Resistance of the Cable	R_g	0.5Ω	0.8Ω
Grid Voltage	v_g	276V	184V
Critical Load	R_c	$R_{c1} = 6.6\Omega$	$R_{c2} = 50\Omega$
Non-Critical Load	R_{nc}	1Ω	2.2Ω
Impedance of Critical Load	Z_c	$6.6 \pm$ j5.78Ω	$50 \pm$ j5.78Ω
Rating of the Inverter (ES)		63.1 KVA	
Switching Frequency of the Inverter	f_{sw}	20 KH_z	
Reference Voltage	v_{ref}	230 V (rms)	

monotopic model (thereby wiping out all uncertainties), using parameters mentioned under the column of Upper Limit (considering only the resistive part of Z_c) of Table. 2.1, has been substituted in (2.6) for deriving the A, B, C, D parameters of the state-space model, which is to be used for the design of the controller in the upcoming Chapters.

$$
\begin{aligned}
A &= \begin{bmatrix} -1.89e4 & -1.67e5 & 1.25e5 \\ 500 & 0 & 0 \\ -2459 & 0 & -7049 \end{bmatrix} ; \\
B &= \begin{bmatrix} 0 & 0 \\ -500 & 0 \\ 0 & 3279 \end{bmatrix} ; \\
C &= \begin{bmatrix} 0.75 & 0 & 1.65 \end{bmatrix} ; \\
D &= \begin{bmatrix} 0 & 0 \end{bmatrix}
\end{aligned}
\tag{2.7}
$$

This derived model of ES (2.7) has been validated through the Matlab (function power_analyze() and corresponding Simulink model).

2.5 Design Consideration of Electric Spring Acting as an Inverter

A Second-generation ES is a Single-phase converter, making possible the bidirectional transfer of power (active and reactive) to regulate the voltage across the critical load. Judicious selection of switches operating therein and their switching frequency is crucial to this inverter's design. These factors decide the output filter's component values and the switching losses taking place in ES. IGBT has been selected as the switches operating in the inverter because it is considered to cater to low to medium power systems.

2.5.1 Selection of switching frequency

Judicious selection of switching frequency is deciding the losses taking place in the switches of the inverter and at the same time the size of the converter by fixing the physical size of the filter parameters of the inverter. Higher switching frequencies lead to the smaller

component values and size of the output filter, but at the same time, it is inducing more losses in the switches at the instance of turn on and turn off instances. A trade-off has to be made in selecting switching frequency to keep the component size smaller and, at the same time, limit the switching losses to a minimum possible extent. A fixed Switching frequency of $20KHz$, using sinusoidal pulse width modulation, has been selected for the application of ES in this work.

2.5.2 Design of DC Bus

A second generation ES is deployed with a pack of batteries to support the voltage injection or absorption, to keep the critical load's voltage well regulated amidst step and transient changes. Further, the voltage is also dependent on the connecting point of the load in the feeder. The fag end faces the lowest voltage due to the drop across the feeder impedance depending on the distribution line's length and its conductor type. A Dog conductor of $1Km$ length (maximum) has been considered, causing a voltage drop of around $45V$ (RMS), in the supposed system (ref. to Fig:2.7).

ES has to support the voltage, such that it behaves as if it is either a variable inductor or a variable capacitor, in the presence of over-voltage and under-voltage scenarios ($v_{ref} \pm$ 20%), respectively. A DC bus having a range-bound voltage variation of 550-750 V has been considered after applying all these considerations.

2.5.3 Design of Output Filter

The output filter's function is to minimize the ripple content in the current and voltage signals inflicted due to high-frequency switching applied to the inverter switches. Various filter variants have been presented in the technical literature (e.g., L, L-C, L-C-L, pi, etc.). Switching frequency harmonics could be attenuated in a much better way by L-C and L-C-L filter when being compared with L filter. However, the L-C-L filter increases the system's order and may cause oscillations in the system by introducing the resonant peaks [74]. L-C filter, attenuate the harmonics being generated by the high-frequency switching of the inverter with small ratings (few KW), is a better choice [75] for the application of ES, which may offer adequate filtration and at the same time keeps the order of the system to a minimum.

2.5.3.1   Inductor Design

The inductor's primary function is to reduce the harmonics in the inverter's output current, being present due to high frequency switching. Current ripple ($\triangle i_{pp}$) minimization is an additional task that has to be considered while carrying out the inductor design. The design procedure mentioned in [76], has been followed to find the value of L_f and the same is briefed here as follows:

Let, the voltage across the inductor "V_l" be,

$$V_l = L_f \frac{di_l}{dt}$$
$$\Rightarrow (V_{dc} - V_{es}) = L_f \frac{\triangle i_{pp}}{DT_s}, \ where, \ T_s = \frac{1}{f_{sw}} \tag{2.8}$$
$$\Rightarrow \triangle i_{pp} = \frac{D(V_{dc} - V_{es})}{L_f f_{sw}}$$

where,

D, is the duty cycle and is given as,

$D(\omega t) = m \cdot sin(\omega t) = \frac{V_{es}}{V_{dc}}$,

substituting the value of D into (2.8) yields,

$$\triangle i_{pp} = \frac{V_{dc} \cdot m \cdot sin(\omega t)(1 - m \cdot sin(\omega t))}{L_f f_{sw}} \tag{2.9}$$

Solving (2.9) for maximum peak to peak ripple, by applying the condition for maxima, yields,

$$\frac{d(\triangle i_{pp})}{dt} = k\{cos(\omega t)(1 - m \cdot sin(\omega t)) - m \cdot cos(\omega t)sin(\omega t)\} = 0$$
$$\Rightarrow sin(\omega t) = \frac{1}{2m} \tag{2.10}$$

Modulation index at the maximum ripple condition can be found from (2.10), and substituting this into (2.8) gets us the value of L_f as,

$$L_f = \frac{V_{dc}}{4 f_{sw} \triangle i_{pp} \mid_{max}} \tag{2.11}$$

The inductor value of $L_f = 2mH$ has been found by substituting the parameters mentioned in Table:2.1 into (2.11) and considering $\triangle i_{pp}$ not to exceed 1.15% of the peak inductor current.

2.5.3.2 Design of Capacitor

The cut-off frequency (f_c) for the Low-pass filter design is having a significant role to play. A rule that gives an idea about the range of frequency for which the filter gives out the satisfactory performance, keeping the component size to a minimum, is presented [76] as,

$$10f_s < f_c < \frac{f_{sw}}{10} \tag{2.12}$$

$$500Hz < f_c < 2000Hz \tag{2.13}$$

Significant switching frequency attenuation could be achieved at the cut-off frequency $f_c = 1439Hz$. By substituting this and the value of L_f in,

$$C_f = \frac{1}{4\pi^2 L_f f_c} \tag{2.14}$$

yields, the value of C_f as $6mF$.

2.5.4 Results of Inverter Design

The designed parameters of the inverter need validation, and the same has been verified through the frequency response of the designed converter.

The frequency response plot can give an idea about the attenuation characteristics of a filter. The designed low pass filter of the VSC has been evaluated for its attenuation characteristics through the frequency response plot being assimilated for the range of loads presented in Table:2.2. These diverse and varied ranges of loads have been decided to be used as critical loads in the simulation test bench of ES, as well.

It can be noticed from the phase and amplitude plot of Fig:2.4 that the frequencies up to ω_s remain unattenuated. A sharp roll-off can be seen for almost all the loads, except for R-L and $R_{c2}(= 50\Omega)$ type of loads. Transient peaks of moderate amplitude can be seen near the cut-off frequency, ω_c. Fig:2.4 is ascertaining and validating designed filter, in terms of its filtering characteristics. Inverter design has further been validated through the simulation of the experimental test bench (shown in Fig:2.14), in the absence of grid connection and closed-loop feedback control system and switching being administered through Sinusoidal Pulse Width Modulation (SPWM) possessing a modulation index of 0.8.

Simulation results have been presented graphically in the form of Fig:2.5 through Fig:2.13, and analytically in the Table:2.2. Nicely filtered but unregulated sinusoidal
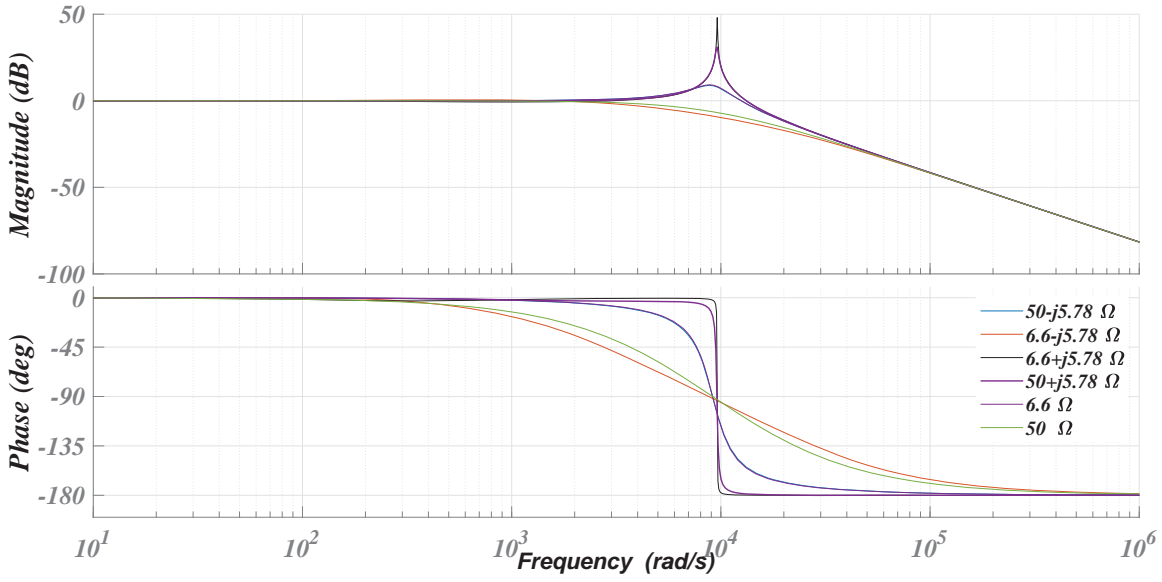
Figure 2.4: Frequency Response Plot of the LC Filter, Tested Against the Prospective Loads of *ES*.
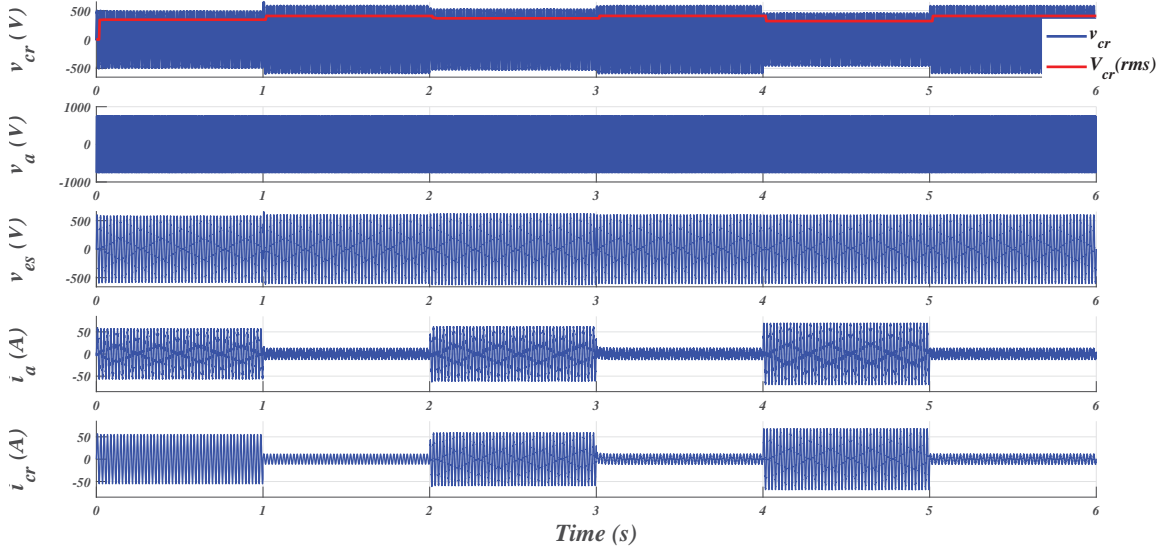

Figure 2.5: Absolute Spectrum of Results Gathered from Test-Bench(0-6s)

waveforms confirm the well-designed filter. Ripple content has been well within the design limits, and the same can be depicted from Fig:2.12. Further, the FFT spectrum, shown in Fig:2.13, of signals associated with the inverter's output and that of the filter, affirms the well-designed filter of the designed inverter.
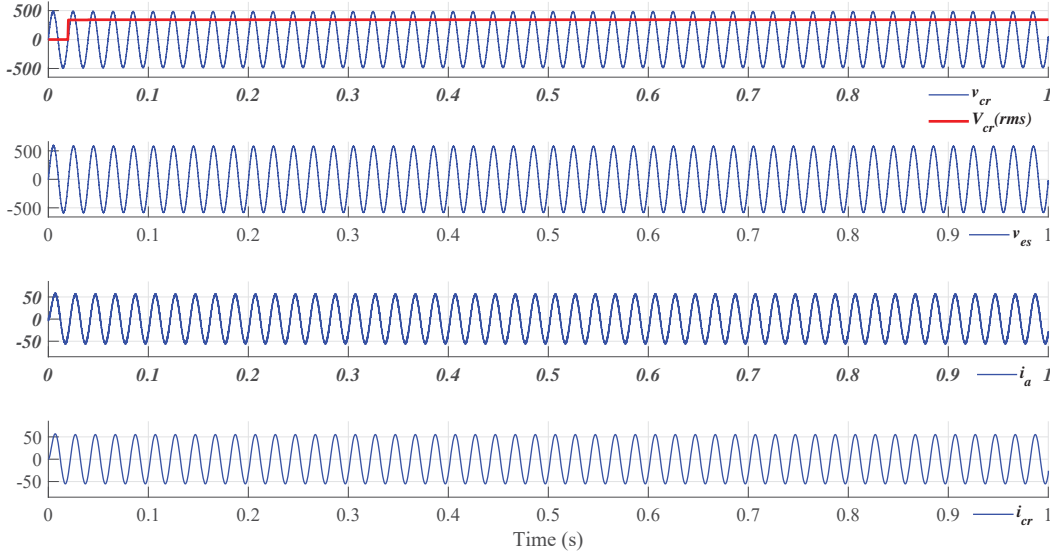
Figure 2.6: Results Associated with R_1-L Load.
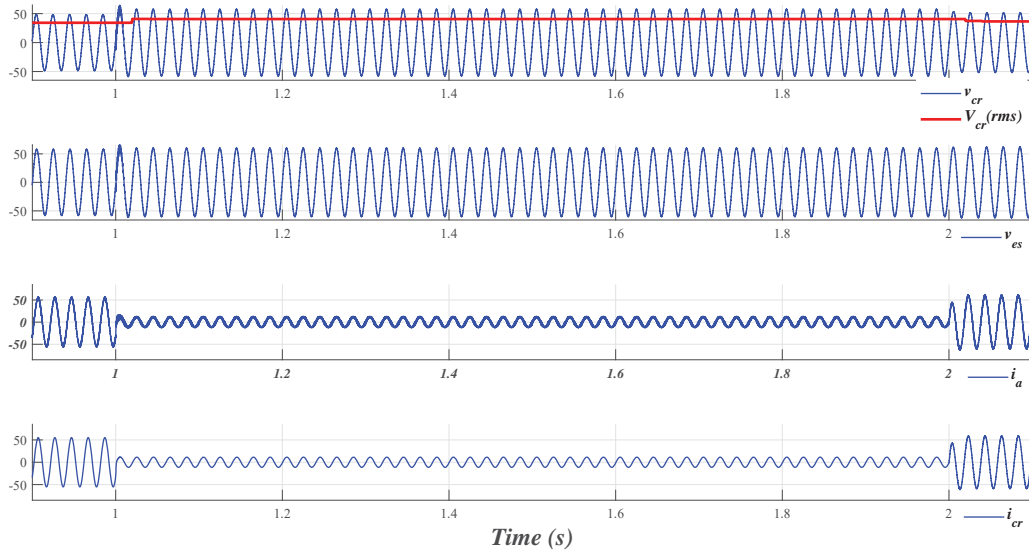
Figure 2.7: Results Associated with R_2-L Load.

2.6   Model of the Grid

The impedance of the distribution grid Z_g (comprising of R_g and L_g) is a parameter of great significance and is dependent on:

- type and amount of the connected load,

- point of the connection,
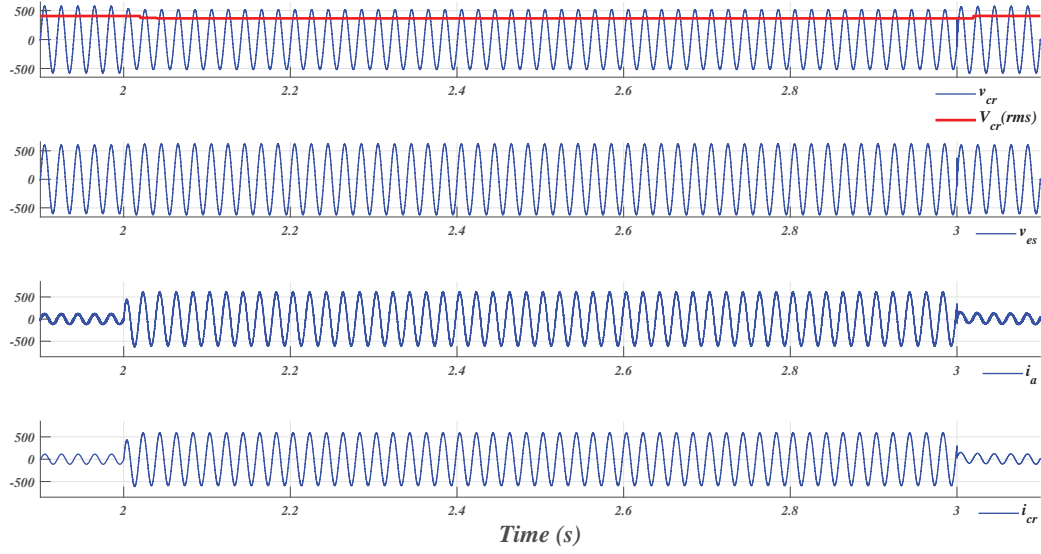
Figure 2.8: Results Associated with R_1-C Load.
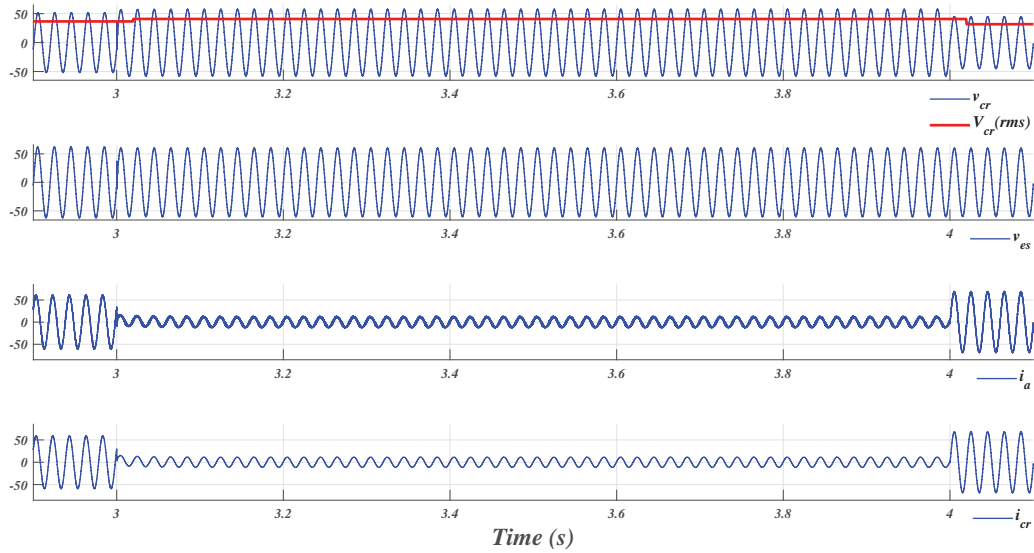
Figure 2.9: Results Associated with R_2-C Load.

- structure of the grid, and

- type of the conductor being used.

Online real-time Estimation of Z_g has lucidly been elaborated in [77][78]. Estimated values could further be updated in the system's model to update the controller being executed using model predictive control (MPC) or sliding mode control, or something of this nature. It has not been presented here in detail for the reason that it is beyond the
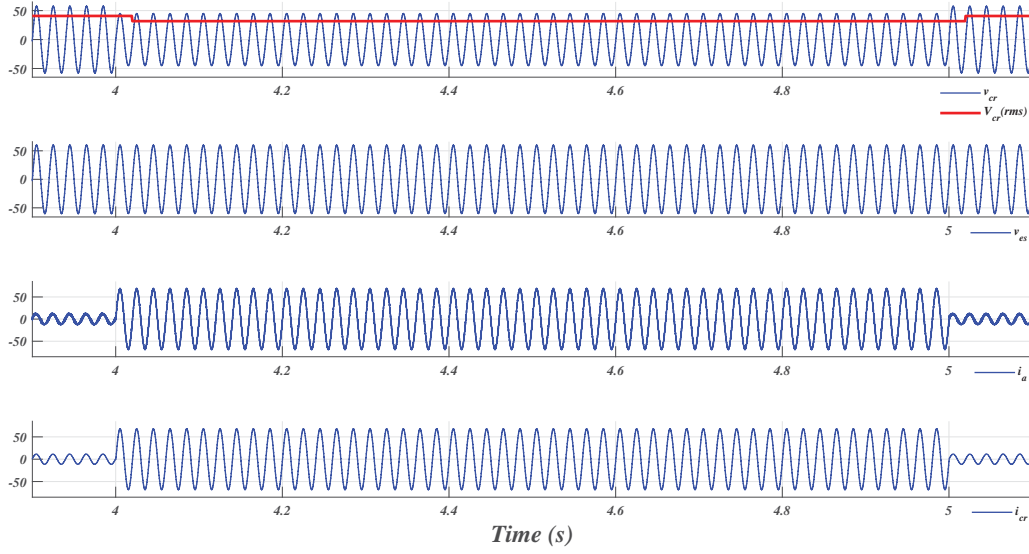
Figure 2.10: Results Associated with R_1 Load.
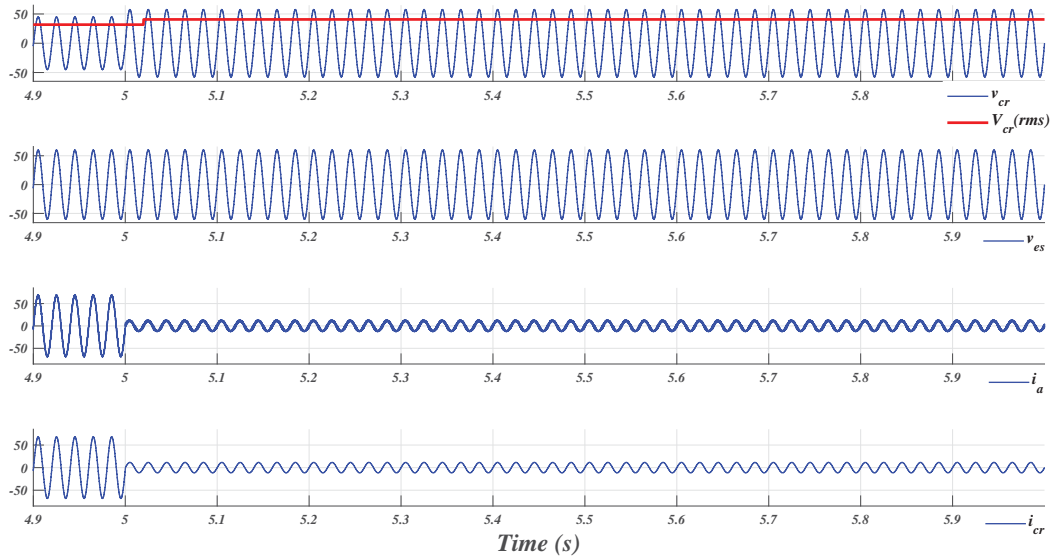
Figure 2.11: Results Associated with R_2 Load.

scope of this work. A stiff grid (where $Z_g < Z_{lf}$, i.e., the impedance of the grid is less than that of a filter inductance) possessing an impedance of $Z_g = 0.5 + j0.1\Omega$ has been considered for non-robust performance analysis. The same has been varied from $0.5 + j0.1$ to $0.8 + j0.3\Omega$ for testing the controller's robustness under the scanner. These values have been deduced from the data of Dog conductor, widely used in the distribution system.
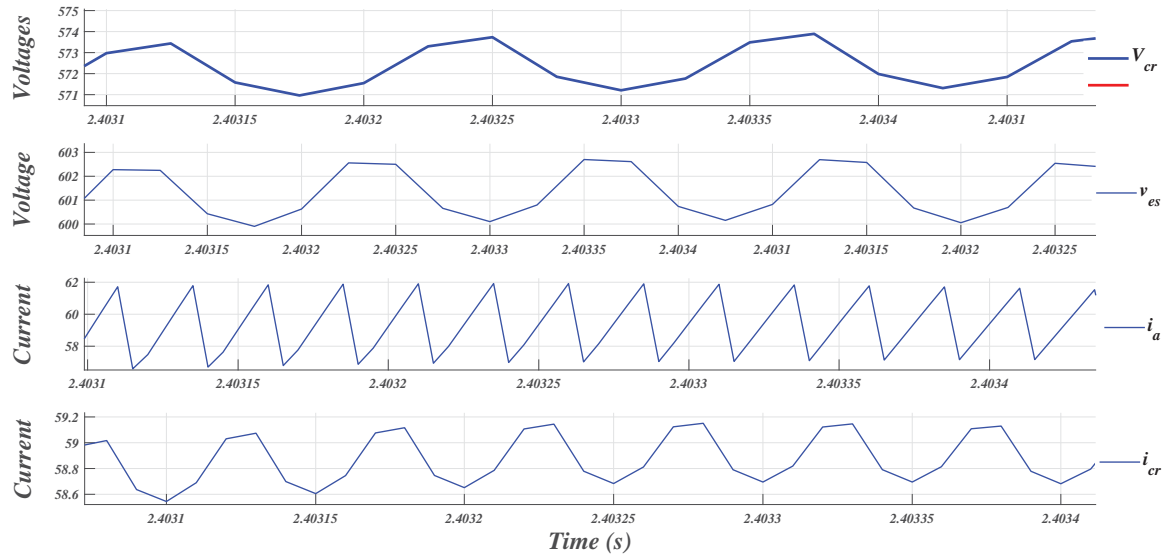
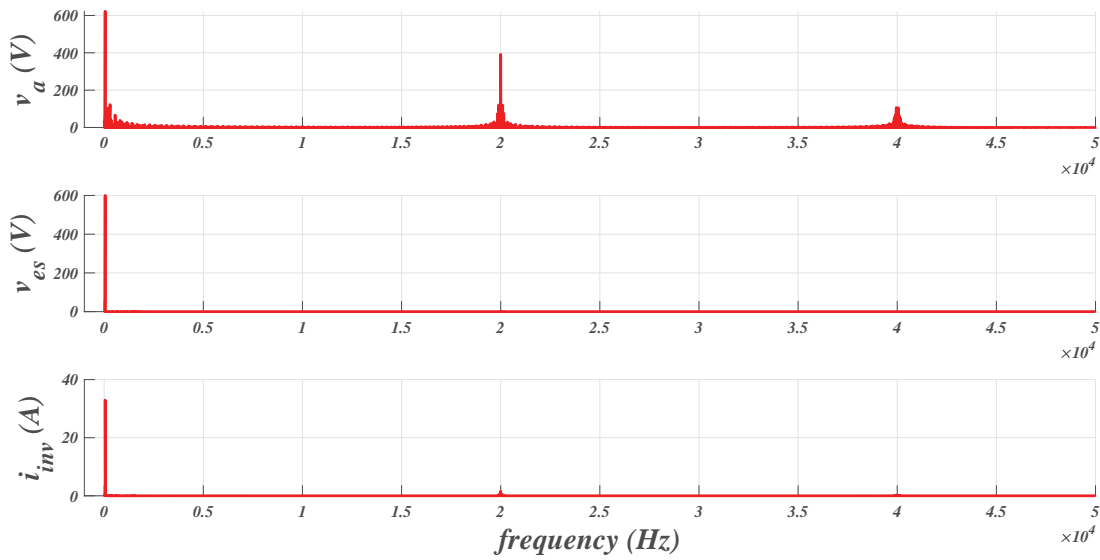Figure 2.12: Spectrum of Results showing the Ripples.

Figure 2.13: FFT spectrum of Results Associated with Inverter.

2.7 Experimental Arrangement for Testing the Performance of the system of ES

A test bench, as shown in Figure. 2.14, has been developed to test the anticipated performance of the system of ES (in the absence of ES, by by-passing it through a shorting link connected across C_f, for the reason that controller of ES has not been introduced

Table 2.2: Results of the Inverter

Time (s)	Load (Ω)	V_a (V)(Peak Value)	RMS Values				% THD				
			$I_a(A)$	$V_{es}(V)$	$V_{cr}(V)$	$I_{cr}(A)$	V_a	I_a	V_{es}	V_{cr}	I_{cr}
0.00-0.99	6.6 + j5.78	750.00	38.69	410.81	342.25	39.06	138.29	5.04	0.61	0.73	0.08
1.00-1.99	50 + j5.78	750.00	8.27	424.23	406.57	8.08	137.85	24.30	0.82	0.86	0.19
2.00-2.99	6.6 - j5.78	750.00	42.24	438.63	365.48	41.74	137.84	4.62	0.57	0.51	0.68
3.00-3.99	50 - j5.78	750.00	8.45	425.33	407.62	8.10	137.88	23.71	0.61	0.61	0.61
4.00-4.99	6.6 + j0.00	750.00	48.12	423.69	317.77	48.08	137.86	4.05	0.59	0.59	0.59
5.00-6.00	50 + j0.00	750.00	8.41	424.74	406.84	8.14	137.84	23.83	0.61	0.61	0.61

yet) under various load variations and voltage excursions in v_g (mimicking a practical situation prevailing in the distribution grid). Grid voltage v_g can be varied here in the range of 184-276V (rms) along with the load that can be varied as different variants viz., R (6.6 Ω, 50 Ω), R-L and R-C(6.6 ± j5.78, 50 ± j5.78Ω) at the different time instances (as mentioned in Table. 2.3), so as to inflict the step changes. Lot of variation in the v_{cr}, v_{nc}, i_g, i_{cr}, and i_{nc} can be seen from the Fig: 2.15 as well as from the Table: 2.3.
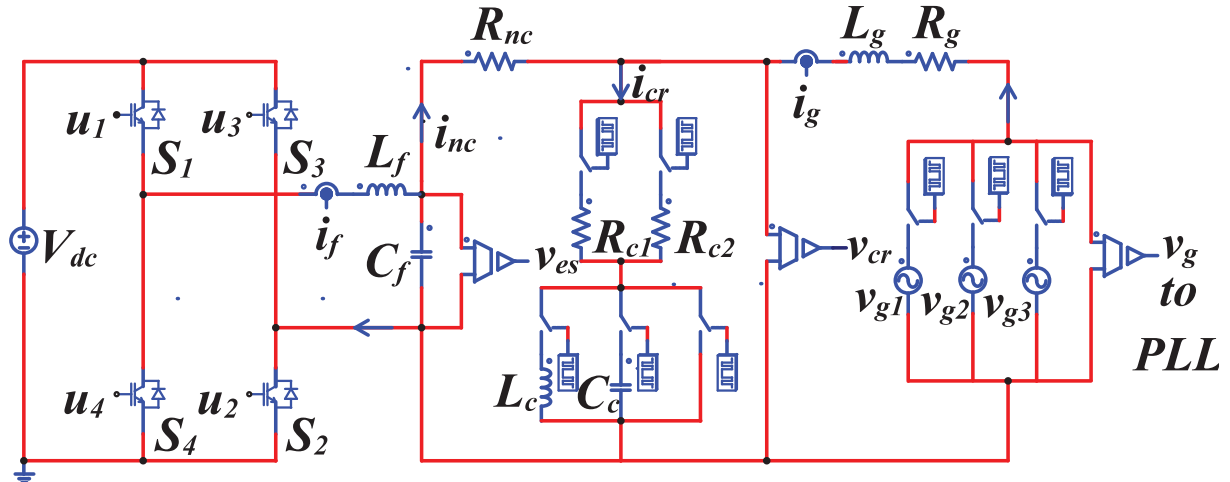

Figure 2.14: Simulation Test Bench of the system of Electric Spring.

This experimental bench has been tested here to perform in the absence of ES. It gives an idea about the variation in system parameters at the wake of step changes applied to grid voltage in the presence of load variations, as has been presented in Table: 2.2, along with its time instances, and the same can graphically be seen from Fig:2.15.
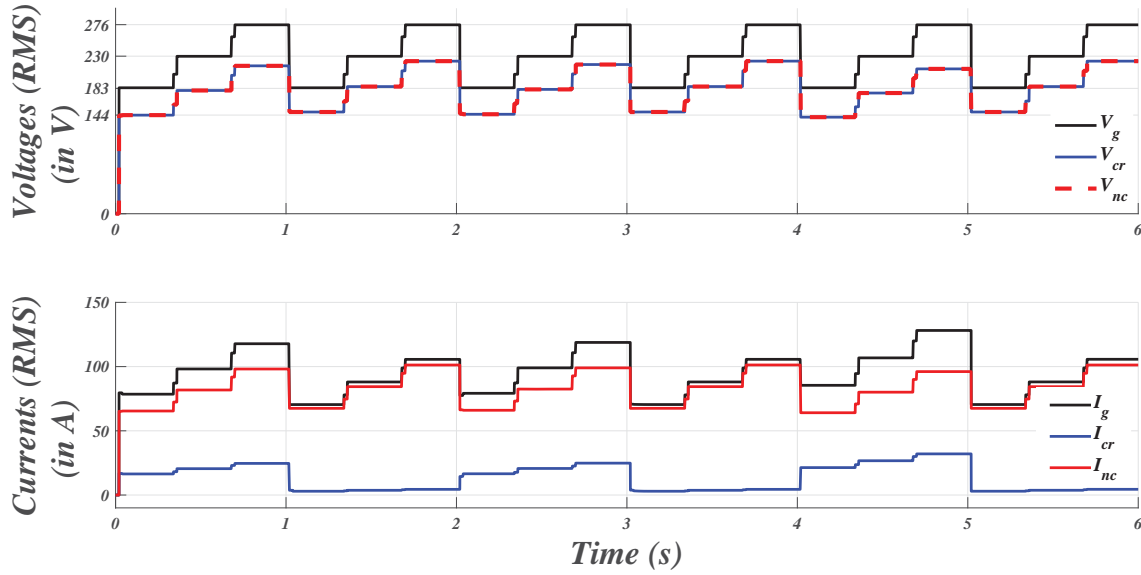
Figure 2.15: Results of the Simulation Test Bench, without the Presence of Electric Spring.

2.8 Conclusion

A primary survey of the *ES* and its basic structure, control, and functioning has been presented in this chapter. The converter's requirements, functioning as *ES*, and its compliance to the standards have been carried out and verified through the simulation results. The designed converter has been performing well to comply with the requirements of power quality standard [66] by keeping the $\%THD < 2\%$.

It is evident from the Fig:2.15, and Table:2.3 that the load and grid voltage variation causes the variation in the voltage across the loads in the range of 144V to little less than 230V. This large and unregulated variation in the critical load voltage (in the range of 3.13% to 38.72%) may not be acceptable. Further, a noticeable change could be seen in the grid current and current flowing through the non-critical load with the change in critical load and grid voltage. Current flowing through the critical load should remain constant as long as the critical load remains constant, no matter what the grid voltage is. Some mechanisms to regulate the critical load voltage and counter the changing current flowing through it must be developed. The answer to these all problems could be found in the form of well-controlled *ES*, which is the upcoming chapters' subject matter.

Table 2.3: Perturbation in the Parameters of the System, in the Absence of ES

Time	*Load*	V_g	V_{nc}	I_{nc}	I_{cr}	I_g	*Power*	V_{cr}	*%Reg.*
(s)	*(Ω)*	*(V)*	*(V)*	*(A)*	*(A)*	*(A)*	*(W)*	*(V)*	V_{cr}
0.00-0.33	6.6 + j5.78	183.85	143.91	65.42	16.41	78.52	11304.70	143.91	-37.43
0.33-0.66	6.6 + j5.78	229.81	179.89	81.77	20.52	98.15	17468.80	179.89	-21.79
0.66-1.00	6.6 + j5.78	275.77	215.87	98.12	24.62	117.78	25144.70	215.87	-6.14
1.00-1.33	50 + j5.78	183.85	148.49	67.49	2.95	70.42	10564.80	148.49	-35.44
1.33-1.66	50 + j5.78	229.81	185.61	84.37	3.69	88.03	16321.70	185.61	-19.30
1.66-2.00	50 + j5.78	275.77	222.73	101.24	4.43	105.64	23493.50	222.73	-3.16
2.00-2.33	6.6 - j5.78	183.85	145.20	66.00	16.55	79.21	11511.60	145.20	-36.87
2.33-2.66	6.6 - j5.78	229.81	181.51	82.50	20.69	99.02	17782.60	181.51	-21.08
2.66-3.00	6.6 - j5.78	275.77	217.81	99.00	24.83	118.82	25596.70	217.81	-5.30
3.00-3.33	50 - j5.78	183.85	148.53	67.51	2.95	70.44	10571.10	148.53	-35.42
3.33-3.66	50 - j5.78	229.81	185.66	84.39	3.69	88.06	16331.00	185.66	-19.28
3.66-4.00	50 - j5.78	275.77	222.79	101.27	4.43	105.67	23507.00	222.79	-3.13
4.00-4.33	6.6 + j0.00	183.85	140.95	64.07	21.36	85.43	12163.50	140.95	-38.72
4.33-4.66	6.6 + j0.00	229.81	176.19	80.09	26.70	106.78	18793.70	176.19	-23.40
4.66-5.00	6.6 + j0.00	275.77	211.43	96.10	32.03	128.14	27052.00	211.43	-8.07
5.00-5.33	50 + j0.00	183.85	148.49	67.50	2.97	70.47	10571.70	148.49	-35.44
5.33-5.66	50 + j0.00	229.81	185.61	84.37	3.71	88.08	16331.90	185.61	-19.30
5.66-6.00	50 + j0.00	275.77	222.74	101.24	4.45	105.70	23508.80	222.74	-3.16